Original article

Folia Neuropathologica

Differentiation between brain tumor recurrence and radiation injury using perfusion, diffusion-weighted imaging and MR spectroscopy

Barbara Bobek-Billewicz[1], Gabriela Stasik-Pres[1], Henryk Majchrzak[2], Łukasz Zarudzki[1]

[1]Department of Radiology, Maria Sklodowska-Curie Memorial Cancer Center and Institute of Oncology, Gliwice Branch, Poland;
[2]Department of Neurosurgery in Sosnowiec, Silesian Medical University, Katowice, Poland

Folia Neuropathologica 2010; 48 (2): 81-92

Abstract

Background: *Differentiation between tumor recurrence/vital tumor tissue and radionecrosis based on conventional diagnostic imaging is impossible because of the likeness of the images. In such circumstances advanced MRI techniques (PWI, DWI, 1HMRS) seem to be helpful. The aim of our study was to evaluate the diagnostic effectiveness of PWI, DWI and 1HMRS in the differentiation of the tumor recurrence from radiation related injury.*

Material and methods: *The retrospective analysis compriesed 11 contrast-enhancing lesions observed in 8 patients treated for gliomas with radiotherapy or radiochemotherapy. 5 out of 11 contrast-enhancing lesions were tumor recurrences whereas 6 out of 11 radiation-related injuries. The MR examinations comprised of conventional MR imaging (T1-SE, T1-MPRAGE with CE, T2-TSE, T2 FLAIR) and PWI, DWI, 1HMRS. Mean and maximum rCBV values of each contrast-enhancing lesion were calculated. These values were normalized to normal appearing white matter. Mean normalized ADC ratio to normal appearing white matter and mean ADC obtained from contrast-enhancing lesions were analysed. In 1HMRS only those voxels which were placed in solid part of the contrast-enhancing lesion were anarlysed and Cho/Cr, Cho/NAA ratios presented.*

Results: *Mean normalized $rCBV_{max}$ (2.44 ± 0.73 for tumor reccurence vs. 0.78 ± 0.46 for radiation injury; $p < 0.001$) and mean normalized $rCBV_{mean}$ (1.46 ± 0.49 for tumor reccurence vs. 0.49 ± 0.38 for radiation injury; $p < 0.005$) were significantly higher in the recurrent gliomas group than in the radiation injury one. It was observed that normalized $rCBV_{max}$ higher than 1.7 and normalized $rCBV_{mean}$ higher than 1.25 is highly indicative for recurrent glioma whereas normalized $rCBV_{max}$ lower than 1.0 and normalized $rCBV_{mean}$ lower than 0.5 is highly indicative for radiation injury. Resutls obtained in DWI and 1HMRS were not statistically significant different between two analysed groups. Mean ADCce: 1.06 ± 0.18 × 10^{-3} mm^2/s for tumor reccurence vs. 1.13 ± 0.13 × 10^{-3} mm^2/s for radiation injury; $p = 0.51$. Mean normalized ADC: 1.55 ± 0.39 × 10^{-3} mm^2/s for tumor reccurence vs. 1.55 ± 0.18 × 10^{-3} mm^2/s for radiation injury; $p = 0.98$. Median Cho/Cr ratio: ($2.16_{min/max}$ [1.67-3.15] for tumor reccurence vs. $1.34_{min/max}$ [1.13-2.37] for radiation injury; $p = 0.15$), median Cho/NAA ratio ($1.9_{min/max}$ [0.86-2.36] for tumor reccurence vs. $2.11_{min/max}$ [0.97 vs. 2.87] for radiation injury; $p = 0.51$).*

Conclusions: *Among the analyzed advanced neuroimaging methods PWI seems to be most reliable in differentiation between tumor regrowth/recurrence and radiation necrosis. In these results mean rCBV is a better differing factor*

Communicating author:
Gabriela Stasik-Pres, Maria Sklodowska-Curie Memorial Cancer Center and Institute of Oncology, Gliwice Branch, Street: Wybrzeże Armii Krajowej 15, 44-101 Gliwice, Poland, phone 693 542 283, e-mail: gabastasik@poczta.onet.pl

than max rCBV. Proton MR spectroscopy (1HMRS) and DWI do not differentiate analyzed groups with statistical significance, despite tendency to lower ADC values in recurrence group than in radiation injury one.

Key words: *recurrence, radiation injury, perfusion weighted imaging, diffusion weighted imaging, MR spectroscopy.*

Introduction

Surgery and radiotherapy are the main methods of a treatment in patients with gliomas. Concomitant radiochemotherapy followed by adjuvant chemotherapy has now become the standard of treatment for patients with malignant gliomas. Postoperative radiotherapy in patients with gliomas improves the results of treatment, but it brings some side effects to the brain [8,14,35,37,39]. Three types of side effects are differentiated taking into account the time of its occurrence: acute (early), subacute (early delayed), late (late delayed) [24,26,38].

Radionecrosis is the end point of radiation injury and the worst adverse effect of the radiotherapy. Radionecrosis generally occurs 3-12 months after radiotherapy but can occur up to years or even decades afterwards. Its developement depends on irradiated brain volume, dose of the radiotherapy and concomitant chemotherapy. The incidence of radionecrosis is higher in patients treated with radiochemotherapy than patients treated with radiotherapy alone. Generally, reported incidence of radionecrosis ranges from 2 to 24% [4,12,18,26,35]. Data on the incidence of radiation necrosis are rather underestimated because of the difficulty in radiological differentiation vital tumor tissue and radionecrosis and rare surgery and biopsies in these patients.

Stereotactic biopsy, if performed, should be imaged-guided biopsy. And because of this neuroimaging plays extremely important role in monitoring the therapy and recurrence of brain tumors. Intralesion heterogeneity of the recurrence which can consist in different proportions from the vital tumor tissue and radionerosis decreases accuracy of biopsy. Advanced MR techniques are essential for taking a representative sampling during biopsy or even it could replace this invasive technique.

Conventional MR techniques, such as T2-weighted and gadolinium-enhanced T1-weighted imaging, have limitations in discriminating tumor recurrence and treatment-induced injury. Radiological pattern of radionecrosis with conventional MR techniques is frequently indistinguishable from that of tumor recurrence. Both lesions are heterogenous mainly hiperintensive on T2-weighted images and show strong, often heterogenous contrast enhancement with surrounding edema and mass effect. Standard imaging recurrence/progression criteria are: increased area of gadolinium uptake on MRI or the appearance of new contrast enhacement lesions but radiation necrosis often looks in the same way.

Advanced MRI techniques and PET examination allow the analysis of tumor or necrotic tissue properties and provide more accurate information on its nature. But differentiation between tumor recurrence/vital tumor tissue and radionecrosis based on diagnostic imaging is still very difficult or sometimes impossible [4-6,18,27,43].

The aim of our study was to evaluate the diagnostic effectiveness of perfusion-weighted imaging (PWI), diffusion-weighted imaging (DWI) and magnetic resonance spectroscopy (1HMRS) in the differentiation of the tumor recurrence from radiation related injury.

Material and methods

Material

The retrospective analysis comprised 11 contrast-enhancing lesions observed in 8 patients (5 females, 3 males, range of age 23-68 years) treated for gliomas with radiotherapy (6/8 patients) or radiochemotherapy with Temozolomide (2/8 patients).

In 2 patients contrast-enhancing lesions were multifocal and appeared in different time during follow-up. All patients had undergone surgical excision of the tumor which histological examination results were as follows: Glioblastoma multiforme WHO IV – 2, Astrocytoma anaplasticum WHO III – 5, Astrocytoma diffusum WHO II/III – 1 (Table I). The time from the end of radiation therapy to appearance of contrast-enhancing lesions ranged from 3 to 70 months (Table I). 5 out of 11 contrast-enhancing lesions were tumor recurrences (those results were histopathologically verified). 6 out of 11 contrast-enhancing lesions were radiation-related injuries (3/6 were

histopathologically verified as radionecrosis and 3/6 disappeared completely during follow-up without any treatment and were classified as non-neoplastic lesion/radiation-related injury). The clinical characterisation of the analysed group is presented in Table I.

Methods

The MR examinations were performed on 1.5T (Avanto, Siemens) or 3.0T (Achieva, Philips) scanner with the standard head coil.

Conventional MR imaging

Conventional MR imaging consisted of T2-weighted images, FLAIR (fluid-attenuated inversion recovery), T1-weighted images before and after CE (contrast enhancement).

1.5T: T1-SE (TR/TE 458/14 ms, Thk/gap 5.0/1.5 mm, FOV 207 × 230 mm, matrix 288 × 320), T1-MPRAGE with CE (TR/TE 1160/4.2 ms, Thk/gap 0.9/0.0 mm, FOV 230 × 230 mm, matrix 256 × 256), T2-TSE (TR/TE 4240/92 ms, Thk/gap 5.0/1.0 mm, FOV 234 × 250 mm, matrix 360 × 512), T2-FLAIR (TI = 2371 ms, TR/TE 8000/89 ms, Thk/gap 5.0/1.0 mm, FOV 199 × 250 mm, matrix 204 × 256).

3.0T: T1-SE (TR/TE 450/13 ms, Thk/gap 5.0/1.0 mm, FOV 230 × 230 mm, matrix 256/512, T1-3D TFE with CE (TR/TE 6.4/2.3 ms, Thk/gap 1.0/0.0 mm, FOV 256 × 256 mm, matrix 256/256), T2-TSE (TR/TE 3000/80 ms, Thk/gap 5.0/1.0 mm, FOV 230 × 184 mm, matrix 306/512), T2-FLAIR (TI = 2500 ms, TR/TE 9000/125 ms, Thk/gap 5.0/1.0 mm, FOV 230 × 182 mm, matrix 217/512).

Perfusion-Weighted Imaging (PWI)

1.5T: EPI spin echo (TR/TE 1400/30 ms, Thk/gap 5.0/1.5 mm, FOV 230 × 230 mm, matrix 128 × 128). 60 data sets were acquired with a time resolution 1 per data set.

3.0T: EPI gradient echo (TR/TE 16/24 ms, flip 7° slice thickness 4.0 mm, intersection gap 0.0 mm, matrix 64 × 128 pixels). 60 data sets were acquired with a time resolution 1 per data set.

Table I. The clinical characterisation of the analysed group

Patient gender, age [years]	Brain tumor location	Histopathological diagnosis	Time between the end of RT and appearing of the contrast-enhancing lesion	Type of contrast-enhancing lesion	Location of the contrast-enhancing lesion to the postoperative cavity (adjacent, distant)
I (M, 42)	Temporal lobe	GBM IV	6 13	Recurrence (I.1) Radiation injury (I.2)	adjacent adjacent
II (F, 34)	Frontal lobe	Anaplastic Astrocytoma WHO III	18 23 23	Recurrence (II.3) Radiation injury (II.4) Radiation injury (II.5)	adjacent adjacent distant
III (F, 68)	Parietal and occipital lobe	Anaplastic Astrocytoma WHO III	7	Radiation injury (III.6)	adjacent
IV (M, 32)	Temporal lobe	Anaplastic Astrocytoma WHO III	5	Radiation injury (IV.7)	adjacent
V (F, 30)	Frontal lobe	Diffuse Astrocytoma II/III	14	Radiation injury (V.8)	adjacent
VI (M, 49)	Temporal lobe	GBM IV	3	Recurrence (VI.9)	adjacent
VII (K, 23)	Frontal lobe	Anaplastic Astrocytoma WHO III	3	Recurrence (VII.10)	adjacent
VIII (K, 30)	Frontal lobe	Anaplastic Astrocytoma WHO III	70	Recurrence (VIII.11)	adjacent

Paramagnetic gadolinium based contrast medium (0.1 mmoL/kg) was injected at with a rate 6.0 mL/sec, followed by administration of 20 mL bolus of saline.

rCBV (relative cerebral blood volume) maps were calculated by postprocessing software delivered by MR systems producer.

Mean and maximum rCBV values of each contrast-enhancing lesion were calculated. rCBV was calculated as follows:

$rCBV_{mean}$ – region of interest (ROI) covered the contrast-enhancing lesion except necrotic part;

$rCBV_{max}$ – ROI in contrast-enhancing lesion was placed within the highest rCBV after visual assessment of the color map.

These values were normalized to normal appearing white matter.

$rCBV_{nawm}$ – ROI in normal appearing white matter (nawm) was placed within normal appearing white matter in the contralateral hemisphere.

Mean normalized $rCBV_{max}$ = $rCBV_{max}/rCBV_{nawm}$ and mean normalized $rCBV_{mean}$ = $rCBV_{mean}/rCBV_{nawm}$ were analysed. ROIs area ranged from 0.2 to 0.4 cm^2.

Diffusion-Weighted Imaging (DWI)

1.5T: EPI spin-echo (TR/TE 3100/99 ms, b = 0.1000 mm^2/s, FOV 230 × 230 mm; matrix 192 × 192 pixels, slice thickness 5.0 mm, intersection gap 1.0 mm).

3.0T: EPI spin-echo (TR/TE, 3080/70 ms, b = 0.1000 mm^2/s, matrix 112 × 256 pixels, slice thickness 4.0 mm, intersection gap 1.0 mm).

ADC (Apparent Diffusion Coefficient) maps were calculated by postprocessing software delivered by MR systems producer.

ADCce – ROI in contrast-enhancing lesion was placed within solid part of the lesion, within the lowest signal intensity after visual assessment of the ADC map.

ADC_{nawm} – ROI in normal appearing white matter was placed within normal appearing white matter in the contralateral hemisphere.

ROIs area ranged from 0.2-0.4 cm^2. Mean normalized ADC = $ADCce/ADC_{nawm}$ ratio and mean ADCce were analysed.

Proton MR spectroscopy (1HMRS)

1.5T: 3D CSI SE: long TE (TR/TE 1300/135 ms), short TE (TR/TE 1300/30 ms), voxel size 10 × 15 × 10 mm, and SVS SE: long TE (TR/TE 1500/135 ms), short TE (TR/TE 1300/30 ms), voxel size 15 × 15 × 15 mm.

3.0T: 3D CSI PRESS: long TE (TR/TE 1083/288 ms), short TE (TR/TE 1083/35 ms), voxel size 15 × 15 × 12 mm, SVS SE: long TE (TR/TE 1083/288 ms), short TE (TR/TE 1083/35 ms), voxel size 10 × 10 × 10 mm.

Only those voxels which were in solid part of the contrast-enhancing lesion were analysed. MR spectroscopy data were evaluated using LC Model version 6.1-4F. Cho/Cr, Cho/NAA ratios were calculated, Lac and Lip were marked as "+" or "–", if standard deviation of their concentrations were less than 20%. Two contrast-enhancing lesions (number I.2 and II.4) lacked of MR spectroscopy.

Statistical analysis

Continuous parameters with normal distribution were presented as mean ± standard deviation (SD). The normal distribution of parameters was tested with Shapiro-Wilk test. Mean differences were tested between two groups (Group I – contrast-enhancing lesions which were recurrent gliomas, Group II – contrast-enhancing lesions which were radiation injuries). The significance of mean differences was tested with a *t*-Student test. Continuous parameters which were located into groups smaller than 5 were compared with the χ^2 test. Statistically significant *p*-levels were assumed as < 0.05 (two-sided). Statistical calculations and analyses were performed with Statistical PL software version 6.1 by StatSoft, Inc.

Results

Mean normalized rCBV values are presented in Table II. Mean normalized $rCBV_{max}$ and $rCBV_{mean}$ normalized $rCBV_{mean}$ were significantly higher in the recurrent gliomas group than in the radiation injury one. Normalized $rCBV_{max}$: 2.44 ± 0.73 for tumor reccurence vs. 0.78 ± 0.46 for radiation injury; $p < 0.001$ (Fig. 1), and normalized $rCVB_{mean}$: 1.46 ± 0.49 for tumor reccurence vs. 0.49 ± 0.38 for radiation injury; $p < 0.004$ (Fig. 2). It was observed that normalized $rCBV_{max}$ higher than 1.7 and normalized $rCBV_{mean}$ higher than 1.25 is highly indicative for recurrent glioma whereas normalized $rCBV_{max}$ lower than 1.0 and normalized $rCBV_{mean}$ lower than 0.5 is highly indicative for radiation injury.

Neither mean ADCce: 1.06 ± 0.18 × 10^{-3} mm^2/s for tumor recurrence vs. 1.13 ± 0.13 × 10^{-3} mm^2/s for radiation injury; $p = 0.51$ nor mean normalized ADC: 1.55 ± 0.39 × 10^{-3} mm^2/s for tumor reccurence vs. 1.55

± 0.18 × 10^{-3} mm^2/s for radiation injury; $p = 0.98$) were not statistically significant different between two analysed groups. Mean ADC values are presented in Table III and Figs. 3 and 4.

Results of MR spectroscopy are presented in Table IV. Neither median Cho/Cr ratio (2.16 min/max [1.67-3.15] for tumor recurrence vs. 1.34 min/max [1.13-2.37] for radiation injury; $p = 0.15$) nor median Cho/NAA ratio (1.9 min/max [0.86-2.36] for tumor recurence vs. 2.11 min/max [0.97 vs. 2.87] for radiation injury; $p = 0.51$) were not statistically significant different between two analysed groups (Figs. 5-6).

Discussion

Differentiating vital tumor tissue (tumor regrowth/recurrence) from radiation injury remains an important and common issue in neurooncology. Surgery and radiotherapy are the main methods of a treatment

Table II. Parameters obtained in PWI

Patient	Contrast-enhancing lesion	Normalized $rCBV_{max}$	Normalized $rCBV_{mean}$
I	Recurrence (I.1)	1.39	0.86
	Radiation injury (I.2)	0.74	0.26
II	Recurrence (II.3)	2.56	2.0
	Radiation injury (II.4)	0.34	0.24
	Radiation injury (II.5)	0.64	0.32
III	Radiation injury (III.6)	1.24	0.78
IV	Radiation injury (IV.7)	0.33	0.2
V	Radiation injury (V.8)	1.42	1.13
VI	Recurrence (VI.9)	3.16	1.34
VII	Recurrence (VII.10)	3.04	1.92
VIII	Recurrence (VIII.11)	2.06	1.2

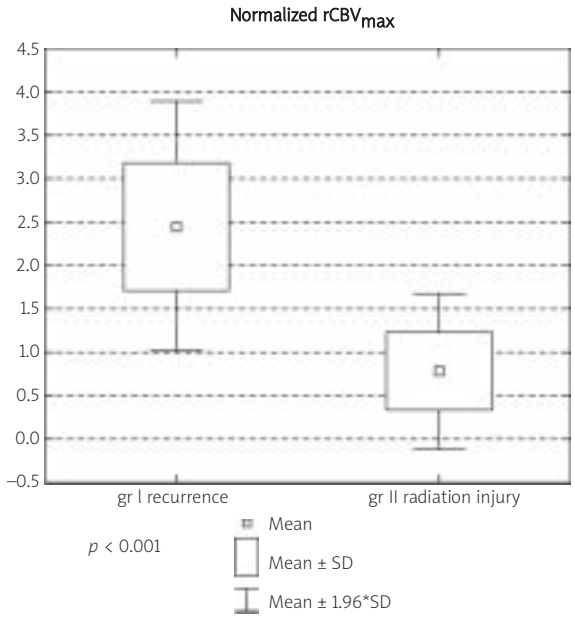

Fig. 1. Box plot of the normalized $rCBV_{max}$.

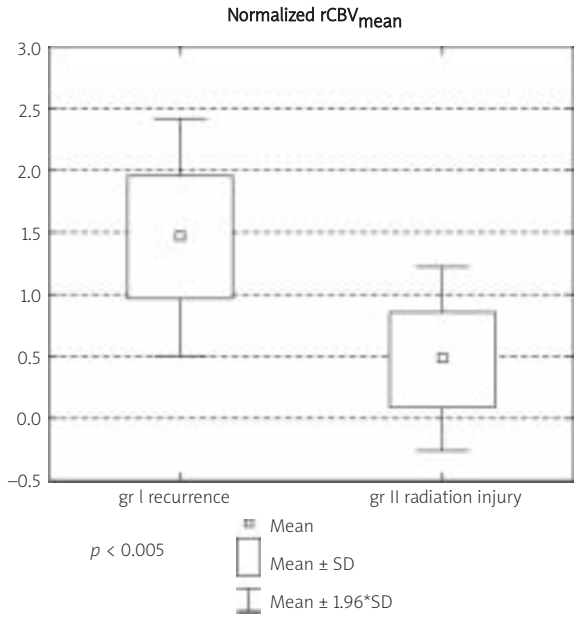

Fig. 2. Box plot of the normalized $rCBV_{mean}$.

Table III. Results obtained in DWI

Patient	Contrast-enhancing lesion	ADCce ± SD [*10-3 mm2/s]	ADC_{nawm} ± SD [*10-3 mm2/s]	Normalized ADC
I	Recurrence (I.1)	0.77 ± 0.14	0.72 ± 0.04	1.06
	Radiation injury (I.2)	1.21 ± 0.74	0.76 ± 0.52	1.59
II	Recurrence (II.3)	1.13 ± 0.03	0.69 ± 0.06	1.64
	Radiation injury (II.4)	1.28 ± 1.05	0.85 ± 0.68	1.51
	Radiation injury (II.5)	1.01 ± 0.84	0.67 ± 0.51	1.52
III	Radiation injury (III.6)	1.24 ± 0.97	0.66 ± 0.50	1.90
IV	Radiation injury (IV.7)	1.10 ± 0.95	0.73 ± 0.39	1.50
V	Radiation injury (V.8)	0.94 ± 0.57	0.71 ± 0.46	1.33
VI	Recurrence (VI.9)	1.08 ± 0.86	0.62 ± 0.47	1.74
VII	Recurrence (VII.10)	1.27 ± 0.03	0.62 ± 0.06	2.05
VIII	Recurrence (VIII.11)	1.07 ± 0.79	0.84 ± 0.37	1.30

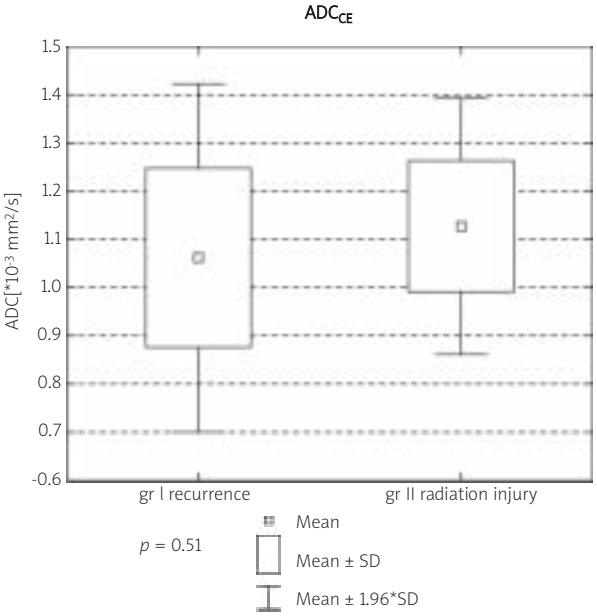

Fig. 3. Box plot of the mean ADC CE.

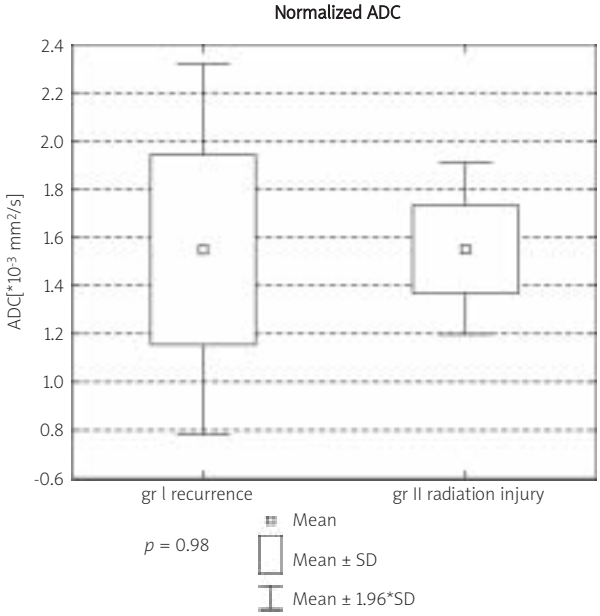

Fig. 4. Box plot of the normalized ADC.

in patients with gliomas. Concomitant radiochemotherapy followed by adjuvant chemotherapy has now become the standard of treatment for patients with malignant gliomas. Postoperative radiotherapy in patients with gliomas improves the results of treatment, but it brings some side effects to the brain [8,14,35,37,39]. Among those radionecrosis – as the end point of radiation injury is the worst. Its developement depends on irradiated brain volume, dose of the radiotherapy and concomitant chemotherapy.

Although radiological features commonly seen in radionecrosis has been described (location in periventricular white matter, corpus callosum and distant from the site of primary tumor, soap bubble, Swiss cheese pattern), differential diagnosis from tumor recurrence based on conventional MR is still impossible [10,18,19], because of the likeness of the

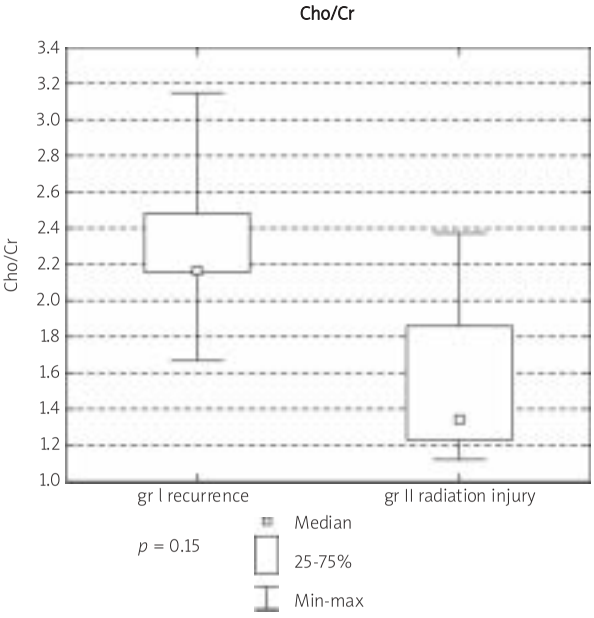

Fig. 5. Box plot of the Cho to Cr ratio.

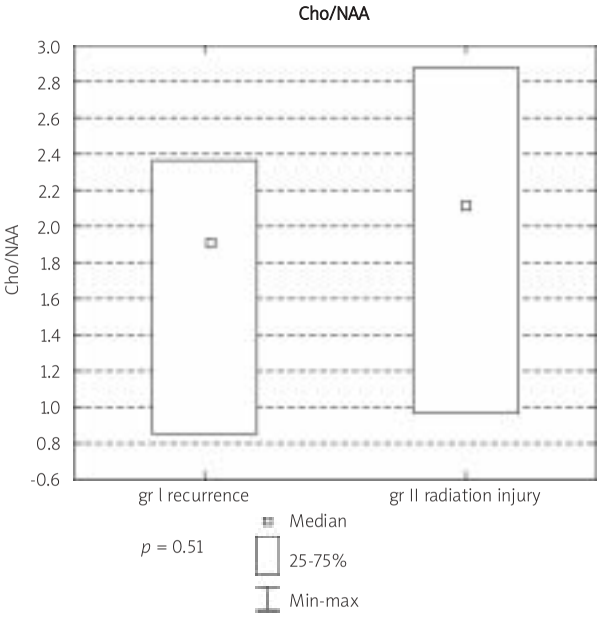

Fig. 6. Box plot of the Cho to NAA ratio.

images. Contrast-enhancing lesions occur within residual tumor or tumor recurrence and also within radiation injuries with or without necrosis [18,25,48]. Both lesions (tumor and radionecrosis) are heterogenous, mainly hiperintensive on T2-weighted images and show strong, often heterogenous contrast enhancement with surrounding edema and mass effect. Both entities can increase in size or be stable over serial examinations. It is essential to

Table IV. Results of MR spectroscopy

Patient	Contrast-enhancing lesion	1HMRS	Cr	Cho	NAA	Lac	Lac + Lip	Cho/Cr	Cho/NAA	Lac and/or Lip
I	Recurrence (I.1)	3D_CSI_TE288ms	$4.57*10^{-4}$	$11.34*10^{-4}$	$1.32*10^{-3}$	$2.31*10^{-3}$	$4.95*10^{-3}$ (1.4-1.3 ppm) $1.73*10^{-3}$ (0.9 ppm)	2.48	0.86	+
II	Recurrence (II.3)	SVS_TE288ms		$29.04*10^{-11}$				#	##	-
	Radiation injury (II.5)	3D_CSI_TE135ms	$1.97*10^{-4}$	$26.64*10^{-5}$	$1.26*10^{-4}$	$1.06*10^{-4}$		1.35	2.11	+
III	Radiation injury (III.6)	3D_CSI_TE135ms	$2.76*10^{-6}$	$3.69*10^{-3}$	$3.81*10^{-6}$			1.34	0.97	-
IV	Radiation injury (IV.7)	SVS_TE135ms	$4.51*10^{-6}$	$10.71*10^{-6}$	$3.73*10^{-6}$			2.37	2.87	-
V	Radiation injury (V.8)	SVS_TE135ms	$2.11*10^{-4}$	$7.14*10^{-4}$				1.13	##	-
VI	Recurrence (VI.9)	3D_CSI_TE135ms	$2.79*10^{-4}$	$4.68*10^{-4}$	$2.45*10^{-4}$	$5.20*10^{-4}$	$6.24*10^{-4}$(1.4 - 1.3 ppm) $2.06*10^{-4}$(0.9 ppm)	1.67	1.9	+
VII	Recurrence (VII.10)	3D_CSI_TE288ms	$1.60*10^{-3}$	$3.45*10^{-3}$		$8.33*10^{-3}$		2.16	##	+
VIII	Recurrence (VIII.11)	SVS_TE135ms	$4.81*10^{-6}$	$10.38*10^{-6}$	$4.40*10^{-6}$		$2.07*10^{-5}$(1.4 - 1.3 ppm)	2.16	2.36	+

SVS – single voxel spectroscopy, CSI – chemical shift imaging, TE – echo time, # only Cho concentration's standard deviation was less than 20%, ##NAA concentration's standard deviation was higher than 20%

remember that from clinical point of view the differentiation between tumor recurrence and radionecrosis has a pivotal role, because of the further treatment implications [4,18].

18 FDG PET/CT (18F-Fluorodeoxyglucose PET/CT) is not a guarantee for reliable diagnosis either. Because of the high physiologic glucose metabolism in normal brain, one faces difficulties in detecting tumor and tumor recurrence. Radiation injuries (especially radionecrosis) are characterized with low FDG uptake. On the other hand small tumor size or its low metabolic activity can be a reason for false negative results. Further, increased FDG uptake in the area of radiation injury can be due to inflammatory processes, seizure activity, healing processes up to 3 months after surgery (false positive results). 18FDG PET/CT has sensitivity 81-86% and specificity 40-94% in differentiation between tumor recurrence and radiation injury [6]. Amino-acid PET e.c. 18F-FET PET (18F(fluoroethyl)-L-tyrosine) seems to be more useful in differential diagnosis. Popperl *et al*. proved that 18F-FET PET was able to distinguish between recurrent tumor and therapy-induced benign changes with 100% accuracy [6,27,43]. In such circumstances advanced MRI techniques (PWI, DWI, 1H-MRS) seem to be helpful in vital tumor tissue vs. benign radiation induced injury/radionecrosis defferentiation.

Dynamic Susceptibility Contrast Enhanced Perfusion MRI (DSCE-MRI, PWI) is based on rapid T2 or T2*-weighted imaging of the first pass of gadolinium-based contrast material. It gives access to information on the capillary microcirculation of tissue and reflects tissue microvascular density (MVD) by measuring relative cerebral blood volume [28,34,46]. The most efficacies, among parametres obtained in PWI, in assessing brain tumors or treatment effectiveness has rCBV [10,19]. Angiogenesis in recurrence/growth tumor lead to raise capillary perfusion and MVD what is seen as an increase of rCBV [16,29]. Tumor's vessels in comparison to normal ones are characterized by increased tortuosity, lack of maturity and increased permeability. MVD and rCBV are decreased in radiation necrosis which mainly consists of ischemic changes because radiotherapy induces endothelial cell damage and small vessel injury [16,29]. Assuming that contrast-enhancing lesion contain pure neoplastic tissue or pure necrotic one, these two entities should be distinguishable by using PWI. But such situation is extremely rare. The areas of recurrence tumor comprised of mixture of neoplastic and necrotic tissue in at least 33% cases [12,26,28]. Because of this overlap of the rCBV between tumor recurrence and radiation injury is predictable. Not only irradiated brain tissue but also irradiated tumor is not the same as before treatment. It was stated [11,42] that normalized rCBV ratios (rCBV[tumor]/rCBV[contralateral tissue]) in the recurrent glioblastoma were significantly lower than those in the initial glioblastoma in the same patients. The usefulness of rCBV in discrimination between tumor reccurence and radiation injury has been evaluated by the same authors. They analysed contrast-enhancing lesions in 20 patients treated with postoperative radiochemotherapy or chemotherapy for gliomas. Estimation showed two thresholds for normalized rCBV ratios – 2.6 and 0.6, respectively. rCBV higher than 2.6 within contrast-enhancing lesions was

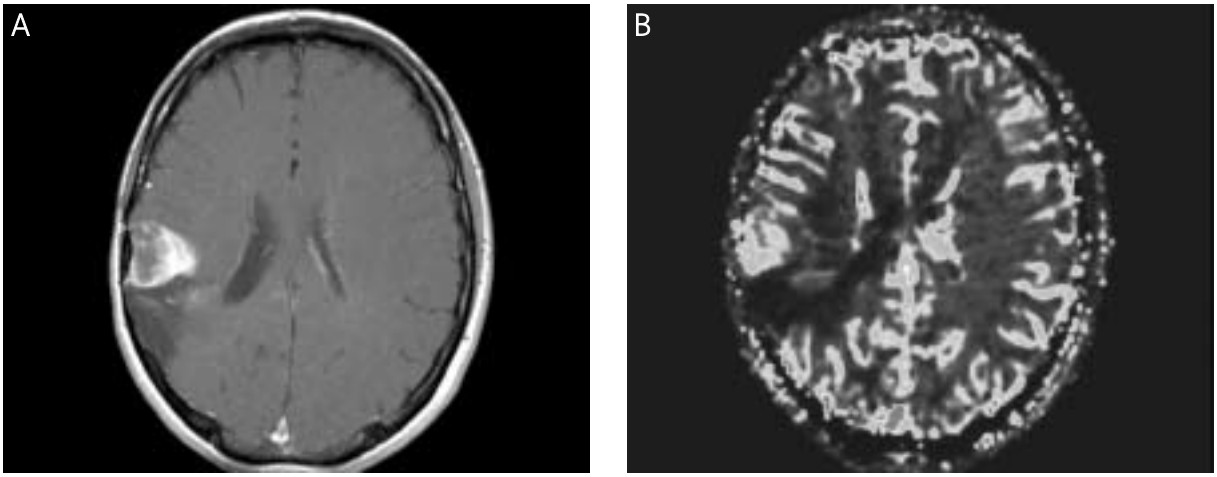

Fig. 7. Recurrent Astrocytoma Anaplasticum WHO III. (A) Contrast-enhancing lesion VIII.11. CE T1-weighted imaging; (B) Contrast-enhancing lesion VIII.11. rCBV map.

highly indicative for tumor recurrence, whereas threshold lower than 0.6 was highly indicative for radiation injury. Values between those two thresholds might have indicated mixture of pathological processes and for better assessment other examinations should have been performed [41,42]. Recently Hu et all. presented a threshold of 0.71 of rCBV with a sensitivity of 91.7% and a specificity of 100% for the best differential diagnosis [16]. Authors of these analysis observed very small overlap between two discussed pathological processes only two tumors rCBV values (8.3% of all investigated samples) fell within the posttreatment radiation effect group range. Authors suggested that such efficient results may be due to preload contrast medium bolus for correctin T1-weighted errors and normalization rCBV to average grey matter and white matter and not only to white matter [16]. Barajas *et al*. found that the mean and maximum rCBV values were significantly higher in the recurrent metastatic tumor group than radiation necrosis [3]. Noteworthy fact is that cutoff for rCBV value of 1.52 with a sensitivity of 91.30% and a specificity of 72.73% was characteristic for recurrent metastatic tumor whereas. rCBV values < 1.35 were only observed in enhancing regions, consistent with radiation necrosis. Our results show statistically significant difference in terms of rCBV between the tumor recurrence and the radiation injury group ($nrCBV_{max}$ $p < 0.001$, $nrCBV_{mean}$ $p < 0.005$). Lesion no VIII 11 in our group was histopahologically verified as recurrent Anaplastic Astrocytoma (Fig. 7). In our group normalized $rCBV_{max}$ over 1.7 and normalized $rCBV_{mean}$ over 1.25 characterized regrowth/recurrence, whereas normalized $rCBV_{max}$ below 1.0 and normalized $rCBV_{mean}$ below 0.5 characterized radiation injury. Like in other authors' results, the overlap between the two groups considering rCBV was also observed. Considering that the overlap is not high this method might be highly indicative for differential diagnosis. Further the overlap of the normalized rCBV between these two groups could have a few reasons, as it was stressed above the most important of these

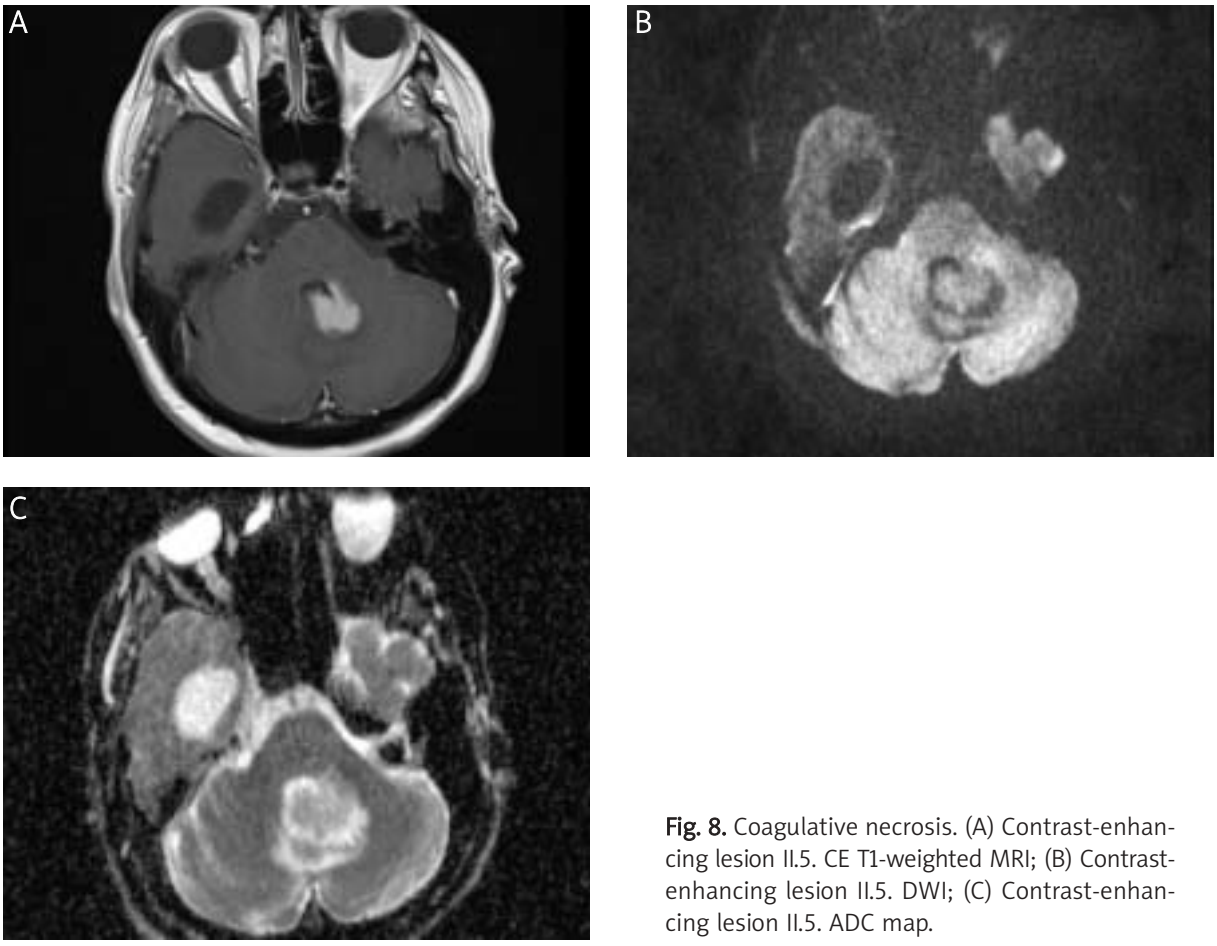

Fig. 8. Coagulative necrosis. (A) Contrast-enhancing lesion II.5. CE T1-weighted MRI; (B) Contrast-enhancing lesion II.5. DWI; (C) Contrast-enhancing lesion II.5. ADC map.

is heterogeneity of the recurrence tumor which often consist of tumor cells and necrosis. Additionally petechial hemorrhage induced by radiation may produce susceptibility artifacts and decrease the rCBV ratios if it occures within tumor recurrence [41,42]. False negative results considering PWI can be similar to problems in FDG PET/CT – small size of tumor and its low metabolic activity. It was observed that within irradiated brain tissue many vessels are occluded but there are aneurysmal formation, teleangiectasias and profliferation of endothelial cells [13,17] what can lead to high perfusion within radiation induced injury/radionecrosis and false positive results.

Extracellular water is the main object of investigation in diffusion imaging. Diffusion data provides indirect information about the structure surrounding these water molecules and is sensitive to microenvironment changes in the tumor and tissue. Quantitative assessment is expressed as ADC maps, which value gets higher if the ability of motion increases. In the opposite if the ability of the water molecules motion is decreased by e.c. the higher cellularity or cytotoxic edema existence, what is called diffusion restriction and what causes diminishing the ADC values. The validity of DWI has been already established in such disorders as acute brain ischemia or differentiation epidermoid vs. arachnoid cyst [33], tumor necrosis vs. abscess and others. Published data regarding ADC changes during the radiotherapy are ambiguous [7,22]. Hein *et al*. showed that ADC ratios (1.43 vs. $1.82*10^{-3}$ mm^2/s) and mean ADC values (1.18 vs. $1.4*10^{-3}$ mm^2/s) in the recurrence group is significantly lower than those of the nonrecurrence group [17]. Similar results presented Zeng *et al*. Authors stated that recurrence group showed mean ADC value and ADC ratio significantly lower than radiation injury group – 1.2 vs. $1.39*10^{-3}$ mm^2/s, 1.42 vs. $1.69*10^{-3}$ mm^2/s, respectively [49]. Interesting analysis presented Asao *et al*. Authors investigated 20 enhancing lesions in which 12 were recurrent tumors and 8 radiation injuries. The minimal, maximal, and mean values of each lesion were compared between these 2 groups. What is noteworthy only the maximal ADC values within each lesion were significantly lower for the recurrence group than for the necrosis one [2]. Our analysis revealed similar tendency to those results but without statistical significance. Contrary results presented Sundgren *et al.* [38] In their group, mean ADC values in the contrast-enhancing lesions were significantly higher for recurrent tumors in comparison with radiation injuries (1.27 vs. $1.12*10^{-3}$ mm^2/s) [47]. It is considered that low ADC values in regrowth/recurrent tumor are the result of high-cell density, but microangiogenesis in the recurrent tumor can elevate ADC values [40]. On the other hand low ADC values in radiation injury could be a result of gliosis, fibrosis, macrophage invasion, demyeliation, coagulative necrosis, but simple acellular necrosis, cystic necrosis, liquefactive necrosis elevate ADC values [49]. Lesion no II.5 in our group was histopahologically verified as coagulative necrosis (Fig. 8). Also, a great deal of recurrent tumors contains areas of necrosis. To sum up, pathological processes within recurrent tumor and radiation injury might lead to similar changes in diffusivity.

MR spectroscopy characterizes tissue in terms of chemical constitution. Taking into account different published reports one may suggest that tumor recurrence may be characterized by high Cho and low NAA levels, whereas radiation injury by low levels of all metabolites, except for lipids [1,9,13,20,23,32,36, 42,45,47,49]. Weybright *et al*. [47] in the group of 29 patients with gliomas treated with surgery and RT noted the highest mean Cho/Cr, Cho/NAA ratios for recurrent tumor, next radiation injury and normal-appearing white matter. Mean NAA/Cr ratio was the highest in normal-appearing white matter, followed by radiation injury, and recurrent tumor respectively [47]. Taylor *et al.* compared absolute concentrations of Cho, NAA and Cr in areas suspected for tumor regrowth or radionecrosis. Authors stated that although for recurrent tumor Cho increase and NAA decrease is highly characteristic, and in radioinjury low levels all these metabolites are seen, discriminant analysis suggested that the primary diagnostic information for differentiating radionecrosis from tumor lay in the normalized MRS peak areas for choline and creatine compounds [44]. According to Zeng *et al*. [49], Weybright *et al.* [47] and Schlemmer *et al.* [36] Cho/Cr ratio > 2 and Cho/NAA ratio > 2.5 in the contrast-enhancing lesions strongly indicate tumor regrowth or recurrence. Rabinov *et al.* [30] stated that the level of Cho at the biopsy site (within contrast-enhancing lesion) to normal creatine level with the treshold greater than 1.3 is the criterion for tumor. Lipids correspond to necrosis which is often visible either within tumor or radiation injury/necrosis. That is the cause that lipids can be detected either in tumor recurrence or radiation injury [31].

Rock *et al*. [32]. Indicated Lac + Lip/Cho ratio = 0.75 as threshold characteristic for tumor recurrence 7 times more often than in radiation injur. Our analysis did not reveal any statistically significant difference between the recurrent gliomas group and radiation injury one in terms of Cho/Cr and Cho/NAA, which can be caused by the small group of analyzed patients. As it has been stated already in many of the enhancing lesions, often both tumor cells and radiation injury are present the results of spectroscopy in these cases are much less clear than those observed in cases of pure tumor or pure radiation necrosis.

Conclusions

Among the analyzed advanced neuroimaging methods PWI seems to be most reliable in differentiation between tumor regrowth/recurrence and radiation necrosis. In these results mean rCBV is a better differing factor than max rCBV. Proton MR spectroscopy and DWI do not differentiate analyzed groups with statistical significance, despite tendency to lower ADC values in recurrence group than in radiation injury one.

References

1. Ando K, Ishikura R, Nagami Y, Morikawa T, Takada Y, Ikeda J, Nakao N, Matsumoto T, Arita N. Usefulness of Cho/Cr ratio in proton MR spectroscopy for differentiating residual/recurrent glioma from non-neoplastic lesions. Nippon Igaku Hoshasen Gakkai Zasshi 2004; 64: 121-126.
2. Asao C, Korogi Y, Kitajima M, Hirai T, Baba Y, Makino K, Kochi M, Morishita S, Yamashita Y. Diffusion-Weighted Imaging of Radiation-Induced Brain Injury for Differentiation from Tumor Recurrence. AJNR Am J Neuroradiol 2005; 26: 1455-1460.
3. Barajas RF, Chang JS, Sneed PK, Segal MR, McDermott MW, Cha S. Distinguishing Recurrent Intra-Axial Metastatic Tumor from Radiation Necrosis Following Gamma Knife Radiosurgery Using Dynamic Susceptibility-Weighted Contrast-Enhanced Perfusion MR Imaging. AJNR Am J Neuroradiol 2009; 30: 367-372.
4. Brandes AA, Tosoni A, Spagnolli F, Frezza G, Leonardi M, Calbucci F, Franceschi E. Disease progression or pseudoprogression after concomitant radiochemotherapy treatment: Pitfalls in neuro-oncology. Neuro Oncol 2008; 10: 361-367.
5. Brandsma D, Stalpers L, Taal W, Sminia P, van den Bent MJ. Clinical features, mechanisms and management of pseudo-progression in malignant gliomas. Lancet Oncol 2008; 9: 453-461.
6. Chen W. Clinical applications of PET in brain tumors. J Nucl Med 2007; 48: 1468-1481.
7. Chenevert T, McKeever P, Ross B. Monitoring early response of experimental brain tumors to therapy using diffusion magneticresonance imaging. Clin Cancer Res 1997; 3: 1457-1466.
8. Combs SE, Widmer V, Thilmann C, Hof H, Debus J, Schulz-Ertner D. Stereotactic radiosurgery (SRS): treatment option for recurrent glioblastoma multiforme (GBM). Cancer 2005; 104: 2168-2173.
9. Czernicki T, Szeszkowski W, Marchel A, Gołebiowski M. Spectral changes in postoperative MRS in high-grade gliomas and their effect on patient prognosis. Folia Neuropathol 2009; 47: 43-49.
10. Danchaivijitr N, Waldman AD, Tozer DJ, Benton CE, Brasil Caseiras G, Tofts PS, Rees JH, Jäger HR. Low-Grade Gliomas: Do Changes in rCBV Measurements at Longitudinal Perfusion-weighted MR Imaging Predict Malignant Transformation? Radiology 2008; 247: 170-178.
11. Di Chiro G, Oldfield E, Wright DC, De Michele D, Katz DA, Patronas NJ, Doppman JL, Larson SM, Ito M, Kufta CV. Cerebral necrosis after radiotherapy and/or intraarterial chemotherapy for brain tumors: PET and neuropathologic studies. AJR Am J Roentgenol 1988; 150: 189-197.
12. Forsyth PA, Kelly PJ, Cascino TL, Scheithauer BW, Shaw EG, Dinapoli RP, Atkinson EJ. Radiation necrosis or glioma recurrence: is computer-assisted stereotactic biopsy useful? J Neurosurg 1995; 82: 436-444.
13. Graves EE, Nelson SJ, Vigneron DB, Verhey L, McDermott M, Larson D, Chang S, Prados MD, Dillon WP. Serial Proton MR Spectroscopic Imaging of Recurrent Malignant Gliomas after Gamma Knife Radiosurgery. AJNR Am J Neuroradiol 2001; 22: 613-624.
14. Grossman SA, Batara JF. Current management of glioblastoma multiforme. Semin Oncol 2004; 31: 635-644.
15. Haymaker W, Ibrahim MZ, Miquel J, Call N. Riopelle AJ. Delayed radiation effects in the brains of monkeys exposed to X- and g-rays. J Neuropathol Exp Neurol 1968; 27: 50-7.
16. Hu LS, Baxter LC, Smith KA, Feuerstein BG, Karis JP, Eschbacher JM, Coons SW, Nakaji P, Yeh RF, Debbins J, Heiserman JE. Relative cerebral blood volume values to differentiate high-grade glioma recurrence from posttreatment radiation effect: direct correlation between image-guided tissue histopathology and localized dynamic susceptibility-weighted contrast-enhanced perfusion MR imaging measurements. AJNR Am J Neuroradiol 2009; 30: 552-558.
17. Hein PA, Eskey CJ, Dunn JF, Hug EB. Diffusion-Weighted Imaging in the follow-up of treated high-grade gliomas: tumor recurrence versus radiation injury. AJNR Am J Neuroradiol 2004; 25: 201-209.
18. Kumar AJ, Leeds NE, Fuller GN, Van Tassel P, Maor MH, Sawaya RE, Levin VA. Malignant Gliomas: MR Imaging Spectrum of Radiation Therapy- and Chemotherapy-induced Necrosis of the Brain after Treatment. Radiology 2000; 217: 377-384.
19. Law M, Young RJ, Babb JS, Peccerelli N, Chheang S, Gruber ML, Miller DC, Golfinos JG, Zagzag D, Johnson G. Gliomas: Predicting Time to Progression or Survival with Cerebral Blood Volume Measurements at Dynamic Susceptibility-weighted Contrast-enhanced Perfusion MR Imaging. Radiology 2008; 247: 490-498.
20. Lichy MP, Henze M, Plathow C, Bachert P, Kauczor HU, Schlemmer HP. Metabolic imaging to follow stereotactic radiation of gliomas – the role of 1H MR spectroscopy in comparison to FDG-PET and IMT-SPECT. Rofo 2004; 176: 1114-1121.
21. Mardor Y, Pfeffer R, Spiegelmann R, Roth Y, Maier SE, Nissim O, Berger R, Glicksman A, Baram J, Orenstein A, Cohen JS, Tichler T.

Early detection of response to radiation therapy in patients with brain malignancies using conventional and high bvalue diffusion-weighted magnetic resonance imaging. J Clin Oncol 2003; 21: 1094-1100.
22. Marcial-Vega VA, Wharam MD, Leibel S, Clark A, Zweig R, Order SE. Treatment of supratentorial high grade gliomas with split course high fractional dose postoperative radiotherapy. Int J Radiat Oncol Biol Phys 1989; 16: 1419-1424.
23. Matulewicz Ł, Sokol M, Wydmanski J, Hawrylewicz L. Could lipid CH2/CH3 analysis by in vivo 1H MRS help in differentiation of tumor recurrence and post-radiation effects? Folia Neuropathol 2006; 44: 116-124.
24. Mishima N, Tamiya T, Matsumoto K, Furuta T, Ohmoto T. Radiation damage to the normal monkey brain: Experimental study induced by interstitial irradiation. Acta Med Okayama 2003; 57: 123-131.
25. Mullins ME, Barest GD, Schaefer PW, Hochberg FH, Gonzalez RG, Lev MH. Radiation necrosis versus glioma recurrence: conventional MR imaging clues to diagnosis AJNR Am J Neuroradiol 2005; 26: 1967-1972.
26. Nieder C, Andratschke N, Price RE, Rivera B, Ang KK. Innovative prevention strategies for radiation necrosis of the central nervous system. Anticancer Res 2002; 22(2A): 1017-1023.
27. Pöpperl G, Götz C, Rachinger W, Gildehaus FJ, Tonn JC, Tatsch K. Value of O-(2-[18F] fluoroethyl)-L-tyrosine PET for the diagnosis of recurrent glioma. Eur J Nucl Med Mol Imaging 2004; 31: 1464-1470.
28. Provenzale JM. Imaging of angiogenesis: clinical techniques and novel imaging methods. AJR Am J Roentgenol 2007; 188: 11-23.
29. Provenzale JM, Mukundan S, Barboriak DP. Diffusion weighted and perfusion MR imaging for brain tumor characterization and assessment of treatment response. Radiology 2006; 239: 632-649.
30. Rabinov JD, Lee PL, Barker FG. In vivo 3T MR spectroscopy in the distinction of recurrent glioma versus Radiation effects: initial experience. Radiology 2000; 225: 871-879.
31. Rock JP, Scarpace L, Hearshen D, Gutierrez J, Fisher JL, Rosenblum M, Mikkelsen T. Associations among magnetic resonance spectroscopy , apparent diffusion coefficients and image guided histopathology with special attention to radiation necrosis. Neurosurgery 2004; 54: 1111-1117.
32. Rock JP, Hearshen D, Scarpace L, Croteau D, Gutierrez J, Fisher JL, Rosenblum ML, Mikkelsen T. Correlations between magnetic resonance spectroscopy and imageguided histopathology, with special attention to radiation necrosis. Neurosurgery 2002; 51: 912-919; discussion 919-920.
33. Rowley HA, Grant P, Roberts T. Diffusion MR imaging. Theory and applications. Neuroimaging Clin N Am 1999; 9: 343-361.
34. Rosen BR, Belliveau JW, Vevea JM. Perfusion imaging with NMR contrast agents. Magn Reson Med 1990;14: 249-265.
35. Ruben JD, Dally M, Bailey M, Smith R, McLean CA, Fedele P. Cerebral radiation necrosis: incidence, outcomes, and risk factors with emphasis on radiation parameters and chemotherapy. Int J Radiat Oncol Biol Phys 2006; 65: 499-508.
36. Schlemmer HP, Bachert P, Herfarth KK, Zuna I, Debus J, van Kaick G. Proton MR spectroscopic evaluation of suspicious brain lesions after stereotactic radiotherapy. AJNR Am J Neuroradiol 2001; 22: 1316-1324.
37. Shaw EG, Daumas-Duport C, Scheithauer BW, Gilbertson DT, O'Fallon JR, Earle JD, Laws ER Jr, Okazaki H. Radiation therapy in the management of low-grade supratentorial astrocytomas. J Neurosurg 1989; 70: 853-861.
38. Shields AF. PET imaging with 18F-FLT and thymidine analogs:promise and pitfalls. J Nucl Med 2003; 44: 1432-1434.
39. Stupp R, Roila F; ESMO Guidelines Working Group. Malignant glioma: ESMO clinical recommendations for diagnosis, treatment and follow-up. Ann Oncol 2008; 19 Suppl 2: ii83-85.
40. Sundgren PC, Fan X, Weybright P, Welsh RC, Carlos RC, Petrou M, McKeever PE, Chenevert TL. Differentiation of recurrent brain tumor versus radiation injury using diffusion tensor imaging in patients with new contrast-enhancing lesions. Magn Reson Imaging 2006; 24: 1131-1142.
41. Sugahara T, Korogi Y, Kochi M, Ikushima I, Hirai T, Okuda T, Shigematsu Y, Liang L, Ge Y, Ushio Y, Takahashi M. Correlation of MR imaging-determined Cerebral Blood volume maps with histologic and angiographic determination of vascularity of gliomas. Am J Roentgenol 1998; 171: 1479-1485.
42. Sugahara T, Korogi Y, Tomiguchi S, Shigematsu Y, Ikushima I, Kira T, Liang L, Ushio Y, Takahashi M. Posttherapeutic Intraaxial Brain Tumor: The value of Perfusion-sensitive Contrast-enhanced MR Imaging for Differentiating Tumor Recurrence from Nonneoplastic Contrast-enhancing Tissue AJNR Am J Neuroradiol 2000; 21: 901-909.
43. Tashima T, Morioka T, Nishio S, Hachisuga S, Fukui M, Sasaki M. Delayed cerebral radionecrosis with a high uptake of 11C-methionine on positron emission tomography and 201Tl-chloride on single-photon emission computed tomography. Neuroradiology 1998; 40: 435-438.
44. Taylor JS, Langston JW, Reddick WE, Kingsley PB, Ogg RJ, Pui MH, Kun LE, Jenkins JJ 3rd, Chen G, Ochs JJ, Sanford RA, Heideman RL. Clinical Value of proton magnetic resonance spectroscopy for differentiating recurrent or residual brain tumor from delayed cerebral necrosis. Int J Radiat Oncol Biol Phys 1996; 36: 1251-1261.
45. Träber F, Block W, Flacke S, Lamerichs R, Schüller H, Urbach H, Keller E, Schild HH. 1H-MR Spectroscopy of brain tumors in the course of radiation therapy: use of fast spectroscopic imaging and single-voxel spectroscopy for diagnosing recurrence. Rofo 2002; 174: 33-42.
46. Weisskoff RM, Belliveau J, Kwong K. Functional MR imaging of capillary hemodynamics. In: Potchen EJ, Jaacke EM, Siebert JE. Magnetic Resonance Angiography: Concepts and Applications. CV Mosby, St. Louis 1992; pp. 473-484.
47. Weybright P, Sundgren PC, Maly P, Hassan DG, Nan B, Rohrer S, Junck L. Differentiation between brain tumor recurrence and radiation injury using MR spectroscopy. AJR Am J Roentgenol 2005; 185: 1471-1476.
48. Van Tassel P, Bruner JM, Maor MH, Leeds NE, Gleason MJ, Yung WK, Levin VA. MR of Toxic Effects of Accelerated Fractionation Radiation Therapy and Carboplatin Chemotherapy for Malignant Gliomas. AJNR Am J Neuroradiol 1995; 16: 715-726.
49. Zeng QS, Li CF, Liu H, Zhen JH, Feng DC. Distinction between recurrent glioma and radiation injury using magnetic resonance spectroscopy in combination with diffusion- weighted imaging. Int J Radiation Oncology Biol Phys 2007; 68: 151-158.